Received: 4 August 2022 | Accepted: 25 October 2022

DOI: 10.1111/2041-210X.14027

Methods in Ecology and Evolution

RESEARCH ARTICLE

Developing nondestructive species-specific tree allometry with terrestrial laser scanning

Atticus E. L. Stovall[1,2] | Anthony Vorster[3] | Ryan Anderson[3] | Paul Evangelista[3]

[1]NASA Goddard Space Flight Center, Greenbelt, Maryland, USA

[2]Department of Geographical Sciences, University of Maryland, College Park, Maryland, USA

[3]Natural Resource Ecology Laboratory, Colorado State University, Fort Collins, Colorado, USA

Correspondence
Atticus E. L. Stovall
Email: atticus.e.stovall@nasa.gov

Funding information
Goddard Space Flight Center, Grant/Award Number: 80NSSC17K0110 and NNH20ZDA001N-BIODIV; U.S. Department of Agriculture

Handling Editor: Ryan Chisholm

Abstract

1. Allometric equations predict organism attributes from simple measurements and underlie many global-scale estimates, from plant productivity to ecosystem carbon stocks. In forests, destructive harvesting of trees in common groups (e.g. plant functional type) or at the species level is necessary to develop allometry but, since sampling is extremely difficult, predictions from these equations have high uncertainty due to low sample size, spatial bias and unrepresentative sampling of tree size. Terrestrial laser scanning (TLS) is a promising remote sensing technology that enables efficient and nondestructive estimates of tree-level structure for developing allometric equations.
2. Here, we nondestructively estimated component biomass of three coniferous tree species (*Pinus ponderosa*, *Pinus contorta* and *Pseudotsuga menziesii*) in Colorado, USA using TLS. We evaluated the suitability for this nondestructive data to be supplanted for destructive data in the development of species-specific allometric equations and compared the prediction accuracy against a commonly used national-scale allometry.
3. We found TLS biomass estimates were consistently more precise across species (RMSE = ~19%) than nation-scale allometry (RMSE = ~39%). Nondestructive biomass estimates from TLS are a suitable addition to or replacement for traditional sampling methods, with indistinguishable biomass predictions across most of the tested diameter range. We further show how TLS can be used to develop allometric equations compatible with airborne LiDAR and other remote sensing variables (e.g. height and crown area), developing generalized biomass predictions from crown area and tree height ($R^2 = 0.87$).
4. The ability for TLS to support the development of nondestructive allometry at a global scale will enable a more nuanced understanding of the drivers of individual tree architecture, while supporting the next generation of biomass remote sensing.

KEYWORDS
3D, allometry, carbon, LiDAR, metabolic scaling theory, *Pinus contorta*, *Pinus ponderosa*, *Pseudotsuga menziesii*, terrestrial laser scanners

This is an open access article under the terms of the Creative Commons Attribution License, which permits use, distribution and reproduction in any medium, provided the original work is properly cited.
© 2022 The Authors. *Methods in Ecology and Evolution* published by John Wiley & Sons Ltd on behalf of British Ecological Society.

1 | INTRODUCTION

Global forest carbon stock estimates (Friedlingstein et al., 2020) are directly dependent on indirect tree-level predictions of biomass carbon (Chave et al., 2014; Saatchi et al., 2011). Field measurements of tree diameter (and sometimes height) are used to predict tree-level standing biomass with predictive models created from a small number of destructively harvested trees (Chojnacky et al., 2014; Picard et al., 2012). The high cost of creating predictive biomass models, or allometric equations, may limit sample size and diameter range, both of which result in unreliable predictions (Chave et al., 2004; Duncanson, Rourke, et al., 2015; Vorster et al., 2020). The local-, national- and global-scale consequences of applying poorly constrained allometry to trees outside of the diameter range intended for forest carbon stock estimates is unclear but remains common practice due to a lack of alternative methods of predicting biomass in large trees. A more reliable method of developing allometric equations (Weiskittel et al., 2015), unrestricted by tree size and number of samples, is needed to update global-scale networks of plot biomass for improved estimates of global forest carbon storage.

Terrestrial laser scanners (TLS) are stationary ground-based light detection and ranging (LiDAR) instruments that collect millions of millimetre precision range estimates from multiple positions. Over the past decade, TLS has become an established method of nondestructively estimating tree-level and forest structure (Calders et al., 2020; Demol et al., 2022). Much of past work has focused on the development of algorithms to measure tree-level attributes such as diameter at breast height (DBH), height and tree-level biomass (Calders et al., 2015; Hopkinson et al., 2004; Lau, Calders, et al., 2019; Momo Takoudjou et al., 2017; Stovall et al., 2017). The most well-studied means of estimating tree volume (and biomass) using TLS relies on 3D cylinder fitting (e.g. quantitative structure models; QSMs; Raumonen et al., 2013). Many studies have highlighted the utility of cylinder fitting, but needleleaf trees consistently have high volume errors since QSM approaches are extremely sensitive to noise and dense foliage (Demol et al., 2021; Hackenberg et al., 2015). One method of estimating tree-level biomass, outer hull modelling (OHM), was developed to overcome errors in cylinder fitting for needleleaf trees and precisely estimated biomass of lodgepole pine trees for the whole tree, trunk, branch and needle components (Stovall et al., 2017). It remains unclear whether OHM can be applied to other needleleaf species and how errors in biomass estimates may vary by species.

TLS has only recently been proposed and assessed as a means of developing nondestructive biomass allometry (Demol et al., 2022; Lau, Martius, et al., 2019; Momo Takoudjou et al., 2017; Stovall et al., 2018)—a critical step in improving airborne and spaceborne calibration and validation (Disney et al., 2019; Stovall & Shugart, 2018) for the highest precision estimates of global carbon stocks (CEOS, 2021). Here, we aim to determine if terrestrial laser scanning can improve or replace destructive calibration data for species-specific allometric biomass equations. We address this question with 41 destructively harvested trees from three species scanned with TLS prior to harvesting. Using a tested (Stovall et al., 2017) and recently improved TLS tree modelling algorithm (OHM), we nondestructively estimated biomass of the trunk and crown components, validating our estimates with field-measured biomass. We developed biomass allometry from both destructively harvested and TLS estimates, comparing the estimates and confidence interval of the scaling coefficients. In addition, we evaluated TLS for developing remote sensing-compatible allometric biomass equations, as described by Jucker et al. (2017). Finally, we evaluated the predictions from TLS allometry in comparison to the commonly used, national-scale Chojnacky et al. (2014) equations of the United States.

2 | METHODS

2.1 | Destructive harvesting and biomass measurements

We destructively sampled 41 trees that were also scanned with TLS prior to harvesting: 10 ponderosa pine (*Pinus ponderosa* var. *scopulorum*), 10 Douglas fir (*Pseudotsuga menziesii* var. *glauca*) and 21 lodgepole pine (*Pinus contorta* var. *latifolia*). We also scanned 19 additional ponderosa pine trees that were not harvested (see Supporting Information). In total, we scanned 60 trees for this study. Ponderosa pine and Douglas fir were sampled at the Ben Delatour Boy Scout Ranch in Larimer County, Colorado and the lodgepole pine were sampled at the Colorado State Forest in Jackson County, Colorado. Permissions for field work were obtained from the Colorado State Forest Service (administered by Colorado State Forest) and Ben Delatour Scout Ranch. Trees were selected that represented the diameter range on site and were free of deformities. Details about the study sites and destructive sampling procedure are documented in previous publications (Stovall et al., 2017; Vorster et al., 2020). We measured dry total above-ground biomass as well as the bole, bark, branch and foliage components. The bole and bark biomass components spanned the main stem from the 30.5 cm (1 foot) stump (excluded from total tree biomass) to where the bole becomes 10.2 cm (4 inch) in diameter. Branches included wood and bark of the main stem above this point and all branches. Foliage was all needles on the tree. In this study, we combined bole and bark components into a single trunk component, and branch and foliage biomass we combined into crown biomass.

2.2 | Terrestrial laser scanning

2.2.1 | Field TLS methods

Terrestrial laser scans were collected using the same procedure outlined in Stovall et al. (2017) with a phase-shift FARO Focus3D 120 unit (ranging error ~2 mm) at a resolution of 6 mm at 10 m distance (~0.6 mrad). Three to four scans were collected per tree from multiple angles to limit occlusion, requiring approximately 3 min per

scan or ~15–20 min per tree. Stovall et al. (2017) estimated that the required field and processing time required for the nondestructive TLS approach was on average ~16 times less per tree than destructive sampling. The latter approach is especially time consuming for large trees. Scan distance from the target tree was approximately 10 m, varying depending on tree size and stand openings. Styrofoam spheres were placed near the target tree as reference objects for scan registration. Near-windless conditions were required for collecting each scan position to ensure errors in the point cloud were minimized.

2.2.2 | TLS preprocessing

Preprocessing of the TLS data was identical to that described in Stovall et al. (2017). In short, we processed all TLS data in Faro SCENE (2015), where registration of multiple scan positions was completed, and the trees of interest were manually segmented from the point cloud (Figure 1). Stray points were filtered in SCENE using the parameters in Stovall et al. (2017; allocation threshold = 10%, distance threshold = 5 mm, grid size = 3×3). Following Stovall et al. (2017), rather than using automated methods, we manually isolated tree point clouds (clipping trees approximately 30.5 cm above-ground) and separated trunk and crown points in Cloud Compare (version 2.11.1) using the segment tool. During this process we visually inspected the point clouds and focused on isolating obvious trunk points. The remaining points were attributed to the crown of the tree. Each tree took 5–10 min to manually preprocess. Finally, each component was exported in ASCII format to be used in the OHM algorithm.

2.2.3 | Tree modelling approach (Stovall et al., 2017)

The OHM method, developed and applied using the R programming language (R Core Team, 2022), was used to nondestructively estimate tree-level volume from TLS data (Stovall et al., 2017). The approach is completed in two stages: (i) trunk modelling and (ii) crown modelling.

The trunk modelling method originally used convex hull peeling (see Stovall et al. (2017) for details) to 'peel' the outer noisy points from (~10 cm) segments of the trunk point cloud. The original version of the OHM method required the user to estimate the number of peeling iterations. The newest iteration of this algorithm relies on a least squares circle fitting approach, included in the original algorithm, requiring no user input. Still, in this updated version of the OHM algorithm, the 'peeling' approach remains. For a single trunk segment, two circle fits are computed. The first circular fit creates a crop region, excluding exterior noise points. A second circle is then fit to the remaining points, providing the final diameter estimate. The newest version of OHM also computes least squares circle fits on much thinner 1–2 cm thin point cloud subsection slices within each larger trunk segment. The benefit of this approach is twofold. First, an individual trunk segment now

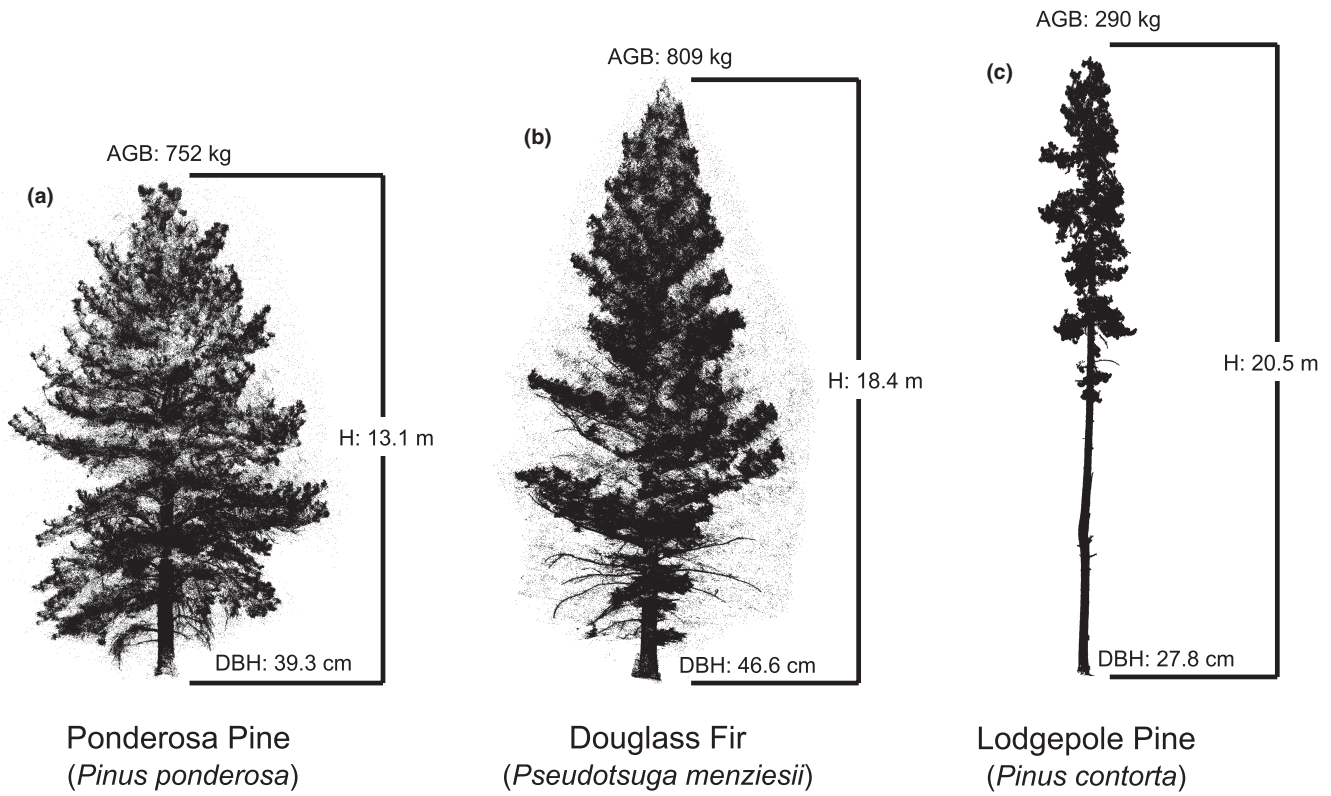


FIGURE 1 Example point clouds highlighting structural differences of the three study species.

has ~10 independent measurements from which a single diameter value is based. Second, the multiple subsection diameters enable confidence intervals for the diameter estimates of individual trunk segments. Next, a linear outlier exclusion method is implemented as described in Stovall et al. (2017), with a plus or minus 20% buffer. Finally, with the remaining diameter values, a median estimate is computed per trunk segment, further reducing the impact of outliers.

The voxel-based branch modelling algorithm is also updated and simplified from the previous version (Stovall et al., 2017). The branch modelling approach is directly dependent on the diameter measurements estimated using OHM. The TLS crown point cloud is voxelized and segmented into 10 cm sections corresponding to the trunk segments. For a given section of crown points the voxel size distribution is adjusted as a log function (B_{model}) based on the OHM estimated trunk segment radius (r):

$$B_{model} = \frac{2r \times \log(D_{max} + 1) - D}{\log(D_{max} + 1)} \quad (1)$$

where D is the distance of the voxel from the trunk and D_{max} is the maximum value of D. Voxels with values of B_{model} less than 1 mm are assumed to be 1 mm in size. For an individual crown subsection, the B_{model} is multiplied by the normalized voxel distribution (total voxels per distance interval from crown normalized by the total number of voxels per crown segment). The approach produces a volumetric distribution of crown points based on adjusted voxel size, which is summed for total crown biomass estimates. The approach differs from the original implementation of the voxel crown modelling in that foliage and branches are not separated from each other. Instead, the modelling is simplified as a single 'crown' volume and biomass. For Douglas fir trees, we found a substantial proportion of TLS returns were attributed to needles along the woody branch structure, dramatically distorting voxel volumes due to an exceptionally high density of returns throughout the crown. The structure of Douglas fir branches is such that the needles account for nearly all branch volume on the exterior portion of the crown. In addition, the beam divergence of laser scanners sets a lower limit of measurable detail at a specific distance (5 mm objects at 10 m distance for the TLS in this study). As a result, the TLS will return near-solid surfaces when measuring these dense needleleaf canopies. To account for these combined measurement challenges, we referenced our available destructive measurements, finding the average ratio between branch and foliage biomass (~0.4 ± 0.1). We applied a simple correction factor of 0.4 times the crown voxel volume, assuming the proportion of returns attributed to needles was 2.5 times more than the returns from branches. We expect a similar approach will be necessary in other high crown density species, requiring further coincident harvest and TLS acquisition. As in Stovall et al. (2017), the final biomass estimates of the trunk and crown components are calculated as the component volume multiplied by average published species-specific wood density values reported in Chojnacky et al., 2014.

2.3 | Developing and comparing Nondestructive Allometry to traditional methods

2.3.1 | Developing Allometric equations

Species-specific allometric equations were developed from both destructive biomass measurements and TLS modelling. We used the *nls* function in R programming language to fit nonlinear models relating DBH (D) in centimetres to total above-ground biomass (AGB) in kilograms using the form:

$$\text{AGB (kg)} = a\,D^{b}, \quad (2)$$

where a is the normalizing coefficient and b is the scaling exponent. We also tested log–log least squares regression (see Supporting Information), but, apart from the error structure, the predictions were not dramatically different from the *nls* model.

In addition, we tested the potential for TLS to aid in the development of remote sensing-compatible allometric relationships as discussed by Jucker et al. (2017). We specifically focused on variables easily derived using high-resolution optical or LiDAR remote sensing methods: (i) crown area and (ii) tree height. We tested the following equation forms as we expected them to be linear in nature, improving prediction stability:

$$\text{AGB (kg)} = \beta_1 + \beta_0 A_{crown}, \quad (3)$$

$$\text{AGB (kg)} = \beta_1 + \beta_0 A_{crown} H, \quad (4)$$

$$\text{AGB (kg)} = \beta_1 + \beta_0 H + \beta_2 A_{crown}, \quad (5)$$

where β_1, β_0 and β_2 are coefficients, A_{crown} is tree crown projected area, and H is tree height. Given the similar wood density across trees in the study, we expected crown structure would explain most of the variation in total biomass. To confirm this expectation, we tested for a species effect in our allometric models but found no significant difference in slope or intercept. We reported the equation coefficients and fit statistics for the final models for Equations (3)–(5).

2.3.2 | Validation and allometric error statistics

The TLS-based tree-level biomass estimates and allometric equation predictions were evaluated using established statistical measures consistent with other similar studies. For all assessments in this study, we derived root mean square error (RMSE; kg and per cent of mean), bias (kg and per cent of mean) and mean absolute error (MAE; kg and per cent of mean). The absolute and relative forms of these statistics allow us to compare within a single species and across species, highlighting differences in error for each category evaluated. For the tree-level validation, we derived these error statistics for comparisons of whole tree biomass, trunk (bole

plus bark) and crown (branch plus foliage) components. For the assessment of allometric prediction errors, we derived the same set of statistics in our evaluation of the errors in whole tree biomass predictions using Chojnacky et al., TLS-derived allometry and TLS tree-level biomass estimates in comparison to the destructively harvested tree biomass data. Additionally, we used fivefold cross-validation (training our allometric models on 80% of the data and holding 20% of data for error estimates) to independently assess prediction errors in the TLS allometry. We used the following DBH-based Chojnacky et al. (2014) equations for our species: Douglas fir (*Pseudotsuga*; 0.45 specific gravity; spg; $\beta_1 = 2.4852$, $\beta_0 = -2.4623$), lodgepole pine and ponderosa pine (*Pinus* <0.45 spg; $\beta_1 = 2.4638$, $\beta_0 = -2.6177$). Component-level predictions were unavailable for Chojnacky et al. equations, so this analysis was excluded from the study.

We highlighted size-dependent differences in errors from our validation of tree-level TLS biomass estimates using one-to-one and residual plots. We highlight the differences in allometry by comparing species-specific predictions using destructive allometry, TLS allometry and the Chojnacky et al. allometry, with confidence intervals shown. We included residual plots to highlight deviations in the TLS allometry and Chojnacky et al. (2014) equations from the destructive allometry. In addition, we showed the comparison between the destructive and TLS allometric coefficients (with confidence intervals) to determine statistical similarity of predictions. Finally, we show trends in absolute errors (kg and per cent of mean) for the TLS allometry and Chojnacky et al. predictions.

3 | RESULTS

3.1 | Whole Tree and component biomass validation

Overall, TLS closely estimated destructive estimates of whole tree, trunk and crown biomass (Table 1; Figure 2). Across the study species, whole tree biomass estimates had relatively low RMSE (13% to 25%) and bias (−4% to 11%). Trunk biomass RMSE ranged from 9% to 32% while bias was −1% to 22%. Crown biomass relative RMSE was higher (17% to 86%) but had low bias (−8% to 4%). Errors in component biomass estimates were dependent on species, with trunk errors lowest in lodgepole pine and highest in Douglas fir, while crown biomass errors were highest in lodgepole pine and lowest in Douglas fir. Ponderosa pine performed well in all whole tree and component estimates (RMSE: 13% to 17%).

3.2 | Comparing destructive, TLS and Chojnacky et al. (2014) Allometry

The TLS-based allometry closely approximated the destructive allometry, with species-specific prediction errors substantially lower than the Chojnacky et al. allometry (Figure 3a; Table 2). The TLS allometry had 4% to 42% lower RMSE and 12% to 30% lower bias than the Chojnacky et al. predictions. TLS allometry predictions were within 3% of the RMSE of the tree-level estimates, except for ponderosa pine, which had ~8% higher RMSE than the tree-level modelling (Table 2). Predictions from the TLS allometry closely approximated the destructive allometry, except in the highest diameter range for a given species. Deviations in predictions occurred above 30 cm for lodgepole pine and Douglas fir, while ponderosa pine remained stable throughout the diameter range. In contrast, the Chojnacky et al. equations deviated at lower diameter ranges and to a greater extent (Figure 3b). The allometric equation coefficients were statistically similar for TLS-based and nondestructive equations (Figure 3c; Table 3). For all normalizing and scaling coefficients (except the scaling coefficient for lodgepole pine) the confidence intervals overlapped with the estimate of the destructive equation. The normalizing coefficients for all species except the destructive allometry were not statistically distinguishable from 0. For ponderosa pine trees, we compared destructive to nondestructive equations, finding negligible differences in the predictions (Figure S3), while the equations of Chojnacky et al. underpredicted. The remote sensing-compatible allometry predicted tree-level biomass across species from crown area and tree height with RMSEs of ~150 to 230 kg or 40% to 60% (Table 4; Figure 4). Mean absolute errors increased with total biomass for both Chojnacky et al. and TLS allometry (Figure 5), but the TLS allometry was consistently more accurate.

TABLE 1 Error statistics from component biomass validation comparing TLS biomass estimates to destructive estimates. PICO, *Pinus contorta*; PIPO, *Pinus ponderosa*; PSME, *Pseudotsuga menziesii*

Component	Species	RMSE (kg)	RMSE (%)	Bias (kg)	Bias (%)	MAE (kg)	MAE (%)
Total	PICO	38.6	20.7	−7.3	−3.9	30.4	16.3
	PIPO	91.8	12.9	17.7	2.5	61.6	8.7
	PSME	70.9	24.8	32.5	11.3	45.3	15.8
Trunk	PICO	12.8	9.1	−1.4	−1.0	10.3	7.4
	PIPO	39.8	13.0	0.5	0.2	26.2	8.6
	PSME	59.7	32.1	40.4	21.8	40.4	21.8
Crown	PICO	34.1	86.1	1.2	2.9	23.5	59.4
	PIPO	69.0	17.1	17.2	4.3	53.1	13.1
	PSME	25.2	25.0	−7.9	−7.9	20.9	20.8

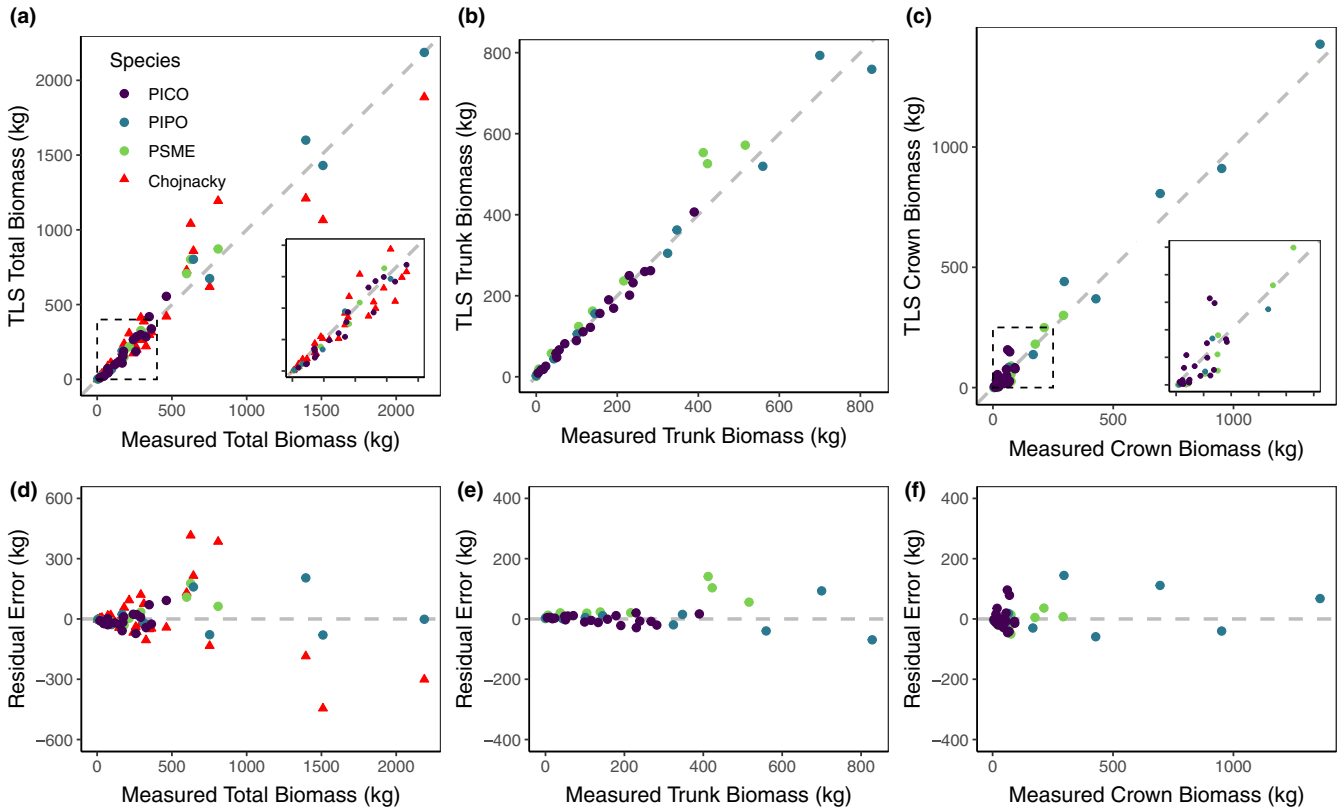


FIGURE 2 Comparison between destructive- and TLS-measured biomass for (a) whole tree, (b) trunk and (c) crown components of the three study species—*Pinus ponderosa* var. *scopulorum* (PIPO), *Pseudotsuga menziesii* var. *glauca* (PSME) and *Pinus contorta* var. *latifolia* (PICO). Chojnacky et al. (2014) Allometric biomass predictions shown in red along the y axis of (a). The dotted grey line is the 1:1 line. Corresponding residual error plots are shown on the bottom row. Insets on panels (a) and (c) correspond to the dotted boxes and show detail in the smaller ranges of biomass.

4 | DISCUSSION

Terrestrial laser scanning is an accurate method of deriving tree-level biomass and is suitable for developing nondestructive allometric equations. In this study, we sought to answer the question, *Can terrestrial laser scanning improve or replace destructive calibration data for species-specific allometric biomass equations?* by extending an established method of tree-level biomass modelling with TLS to the development of allometric equations and comparing our allometric estimates to a commonly applied national-scale biomass allometry. Overall, TLS effectively replaced destructive sampling for three ecologically and commercially important coniferous tree species. We have confidence that this trend will extend to many similarly structured coniferous tree species in dry environments of the western US. In summary, we found the following main takeaways:

1. Outer hull modelling can effectively be extended to additional coniferous species for minimally biased tree-level biomass estimates.
2. Errors in TLS biomass estimates are species and component dependent, requiring further validation when applying the OHM method to new species.
3. TLS can reliably be used to improve or replace traditional methods of allometric biomass equation development.
4. Tree-level remote sensing-compatible allometry can be derived from TLS measurements.

OHM accurately estimated total and component biomass for three common coniferous species. Whole tree biomass was most accurate in ponderosa pine, followed by lodgepole pine and Douglas fir. The pine species biomass estimates were nearly unbiased, while Douglas fir was positively biased by ~11%. Since the diameter range of the study species varied by ~30 cm we cannot rule out the possibility of errors being driven by equation diameter range (e.g. larger trees naturally have more variability in biomass due to plasticity to environmental conditions), especially since the lowest RMSE species had the highest maximum tree diameter (~62 cm). Trunk biomass error was strongly dependent on the crown density of a particular species. Douglas fir trees had extremely high crown density, increasing occlusion of the internal trunk structure and reducing biomass precision. Lodgepole and ponderosa pine had more open crown structure, resulting in less occlusion of the trunk and increased biomass precision. Overall, trunk biomass estimates are extremely reliable—expanding the OHM method beyond the species currently

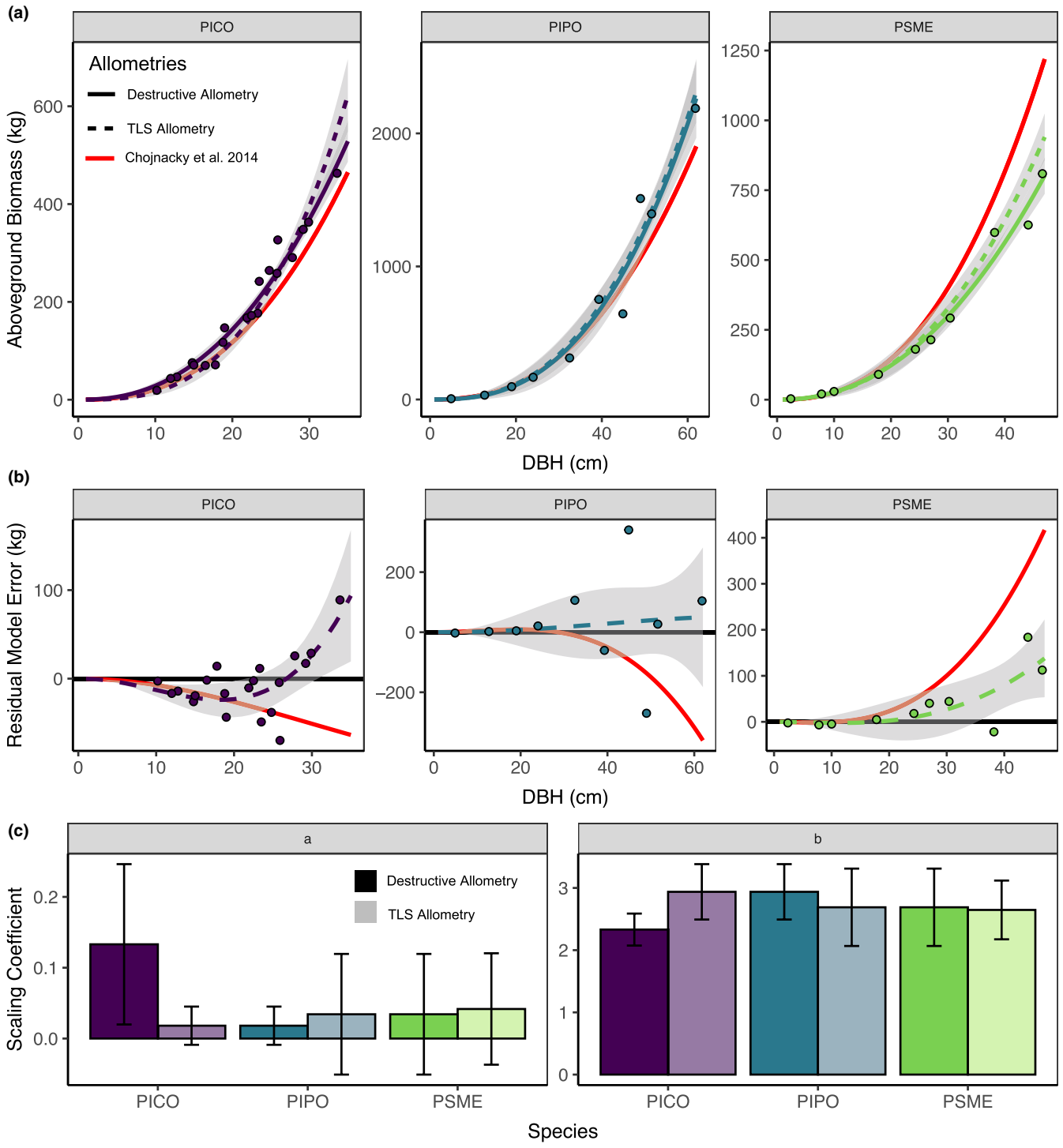


FIGURE 3 (a) Comparison between destructive- and TLS-derived biomass allometry for the three study species—*Pinus ponderosa* var. *scopulorum* (PIPO), *Pseudotsuga menziesii* var. *glauca* (PSME) and *Pinus contorta* var. *latifolia* (PICO)—with allometric model confidence intervals shown in shaded grey. (b) Residual model error (in comparison to the destructive allometric model) shown to highlight deviations from the expected predictions. (c) A comparison between the corresponding destructive (dark) and TLS-derived (light) coefficient estimates (Equation 3) with parameter confidence intervals (error bars) shown on the bottom row.

considered should be reliable, assuming the crown structure is open enough to reduce trunk occlusion in the TLS scans. We expect further improvements to trunk biomass estimates when applying the method to higher-quality multiple-return TLS data that reduces occlusion in the interior crown.

Crown biomass errors were dependent on species-specific crown structure. Ponderosa pine crowns had the lowest noise in the TLS data of any species due to the openness of the crown and relatively heterogeneous clumped needle structure. As a result, these trees had remarkably low errors across all components. In contrast,

TABLE 2 Statistics comparing direct tree-level TLS biomass, TLS nondestructive allometric predictions, and Chojnacky et al. allometric predictions to tree-level destructive biomass estimates. Error estimates from independent fivefold cross-validation shown in parentheses for TLS allometry

Species	Biomass estimate	RMSE (kg)	RMSE (%)	Bias (kg)	Bias (%)	MAE (kg)	MAE (%)
PICO $n = 21$	TLS Modelling	38.6	20.7	−7.3	−3.9	30.4	16.3
	TLS Allometry	33.5 (44.6)	17.9 (23.9)	−6.3 (5.7)	−3.4 (3.1)	24.9 (31.8)	13.4 (17.0)
	Chojnacky	40.5	21.7	−28.8	−15.4	31.1	16.6
PIPO $n = 10$	TLS Modelling	91.8	12.9	17.7	2.5	61.6	8.7
	TLS Allometry	147.0 (185.3)	20.7 (26.1)	28.1 (36.7)	4.0 (5.2)	94.1 (122.8)	13.3 (17.3)
	Chojnacky	198.3	27.9	−74.8	−10.5	138.6	19.5
PSME $n = 10$	TLS Modelling	70.9	24.8	32.5	11.3	45.3	15.8
	TLS Allometry	71.9 (49.6)	25.1 (17.3)	37.0 (−0.2)	12.9 (−0.1)	44.1 (29.0)	15.4 (10.1)
	Chojnacky	190.9	66.7	120.7	42.2	123.1	43.0

TABLE 3 Comparison of allometric coefficients derived from destructive and TLS allometry

Species	Coefficient	Allometry	Estimate	Standard error
PICO	a	Destructive	0.1330	0.0578
		TLS	0.0184	0.0140
	b	Destructive	2.3309	0.1311
		TLS	2.9324	0.2273
PIPO	a	Destructive	0.0184	0.0140
		TLS	0.0343	0.0435
	b	Destructive	2.9324	0.2273
		TLS	2.6889	0.3173
PSME	a	Destructive	0.0343	0.0435
		TLS	0.0427	0.0405
	b	Destructive	2.6889	0.3173
		TLS	2.6410	0.2375

lodgepole pine crowns had a high density of needles on the external portion of the crown structure, occluding the internal branching structure. Although crown biomass RMSE was high in this species, estimates were nearly unbiased, suggesting whole tree biomass estimates should remain unbiased if the method were applied to nondestructively measured trees. Douglas fir crowns had a crown structure with a high density of needles covering all branches, resulting in nearly 2.5 times higher than expected crown volume using the voxel-based algorithm and requiring a correction factor derived from the average ratio of needle to branch biomass (~0.4). The deviation was consistent throughout the range of observed crown biomass, suggesting a simple species-specific correction factor can appropriately adjust these estimates and be applied to other trees within this species. We expect laser scanners with larger beam divergence (e.g. handheld and mobile LiDAR) will suffer greatest from this issue and care should be taken if applying the OHM algorithm. Future studies should not only investigate the consistency of this correction factor for Douglas fir trees but also evaluate the need for correction factors in other species displaying similar high-density needle structure along branches of the tree. Although we did not test quantitative structure models in this study, we expect poor performance in line with Stovall et al. (2017). TLS campaigns targeting single trees (multiple scans around a single individual) should still be paired with destructive sampling as species-specific TLS algorithms continue to be developed and refined to better estimate crown biomass.

The TLS allometric coefficients closely approximated those developed from destructive data, suggesting this method can soon be applied operationally for developing high sample-size biomass allometry including large trees. In contrast, the Chojnacky et al. equations both under (lodgepole and ponderosa pine) and overestimated (Douglas fir) tree-level biomass, with bias increasing with tree diameter and ranging from −16% to 42% (Figure 3; Table 2). The trend of bias in allometric estimates is consistent with past work that found a ~25% underestimate in broadleaf species in comparison to TLS (Stovall et al., 2018). For context, the tree species evaluated here are well characterized since they have commercial forestry value. Prediction errors in species that are less well studied are likely to be substantially higher. For example, a recent study found allometric equations for redwood *Sequoia sempervirens* had ~30% to 40% underestimate in biomass in comparison to TLS (Disney et al., 2020). We expect these trends of biased allometry to continue to emerge with additional TLS-based studies.

The detailed 3D tree-level measurements collected from TLS helps support the development of a new class of remote sensing-compatible allometry. Here, we derived simple attributes directly from the TLS data (e.g. crown diameter and tree height), developing biomass estimates across species with 150 kg or 40% RMSE. Expanding this approach to larger trees will help characterize the uncertainty of these equations, but we expect—like other TLS measures—prediction errors will not be strongly dependent on tree size (Calders et al., 2015; Stovall et al., 2018). Tree-level remote sensing-centric allometry (Jucker et al., 2017), such as this, can be directly applied to optical data using deep learning methods (Weinstein et al., 2021) or to airborne LiDAR data using crown

TABLE 4 Comparison of remote sensing-compatible allometric models. Coefficients are for Equations (3)–(5)

Model	Coefficient	Estimate	SE	R^2	RMSE	RMSE (%)
Crown Area	B1	34.99	40.33	0.71	227.3	60%
	B0	1.99	0.16			
Tree Height × Crown Area	B1	13.72	30.04	0.84	171.0	45%
	B0	0.15	0.01			
Tree Height + Crown Area	B1	29.42	27.00	0.87	150.9	40%
	B0	−1.89	0.46			
	B2	0.27	0.03			

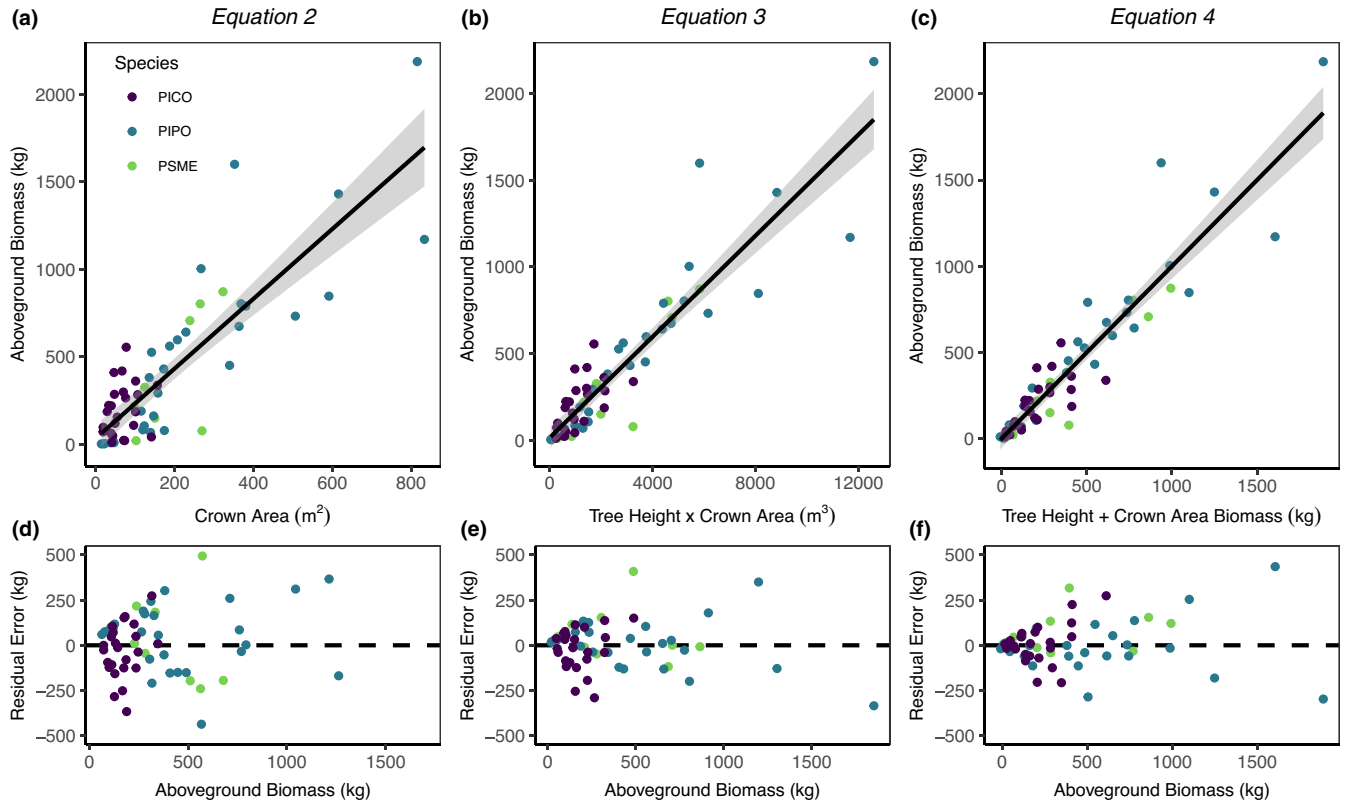


FIGURE 4 Nondestructive remote sensing-compatible biomass allometry developed with TLS estimates of (a) crown area and/or (b and c) tree height. Respective residual plots (d)–(f) are shown on the bottom row.

detection algorithms (Stovall et al., 2019), with immediate applications to high-certainty crown delineation in coniferous forests. Although optical and airborne LiDAR are unable to fully capture understorey trees due to occlusion, the easily measured canopy trees dominate the biomass of many conifer forests (Brown et al., 1997; Stephenson et al., 2014) which is explained primarily by the dominance of stand-replacing disturbance (Lutz et al., 2012). TLS should continue to be integrated into destructive sampling campaigns and leveraged for next generation allometric equations that will allow for precise tree-level biomass predictions, directly relevant to the scale of forest management decisions (i.e. the individual tree).

A key aspect of tree growth is adaptation to environmental conditions, but most species-specific tree-level biomass allometry is unable to incorporate such factors due to a low number of tree observations. Here, adding an additional 19 scanned ponderosa pine trees produced similar biomass predictions, but the increased sample size provided more representative estimates of species-specific variation (Figure S3). Tree-level biomass samples commonly represent a small area and a narrow range of a species' environmental conditions. Past work has investigated environmental drivers of tree allometry (Duncanson, Dubayah, et al., 2015) finding continental variation in scaling relationships, but those studies focused on simple tree-level structural data (height and diameter). Chave et al. (2014) described a single parameter (E) representing variations in environmental stress at a pantropical scale—an approach that could be applied at a finer spatial scale. This represents a key area of future research in tree-level allometry that can only be addressed with massive-scale sampling of whole tree above-ground

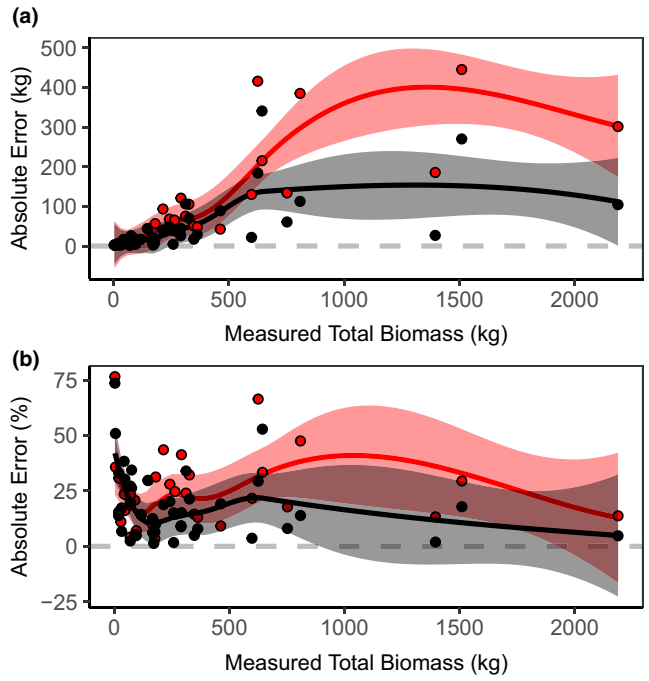


FIGURE 5 Comparison of absolute errors for Chojnacky et al. (2014; red) TLS-derived (black) biomass allometry. Loess smoothing and confidence interval (±1.96 times the standard error of the local loess slope estimate) is shown to visualize the trends in errors.

structure—a goal that can be accomplished with TLS. Understanding the key environmental drivers of tree structure will improve a suite of forest structure-dependent variables, from updated ecological theory to global carbon cycle modelling.

AUTHOR CONTRIBUTIONS

Atticus Stovall, Anthony Vorster and Ryan Anderson developed the study. Ryan Anderson and Anthony Vorster planned and carried out the field work. Ryan Anderson processed the TLS data. Atticus Stovall developed the OHM algorithm and conducted all analyses in the study. Atticus Stovall led the writing of the manuscript. All authors edited the manuscript and gave final approval for publication.

ACKNOWLEDGEMENTS

We thank Ben Delatour Scout Ranch and Colorado State Forest for allowing research access. The study was funded by the Agriculture and Food Research Initiative Competitive Grant (Grant number 2013-68005-21298) from the USDA National Institute of Food and Agriculture. A.S. was funded by the NASA Postdoctoral Program Fellowship and the NASA Biodiversity Program (NNH20ZDA001N-BIODIV). This work was also supported by the USDA National Institute of Food and Agriculture, McIntire Stennis project COL00519, accession 1022909.

CONFLICT OF INTEREST

The authors declare no conflict of interest.

PEER REVIEW

The peer review history for this article is available at https://publons.com/publon/10.1111/2041-210X.14027.

DATA AVAILABILITY STATEMENT

All code for the OHM algorithm is available on GitHub (https://github.com/aestovall/OHM) or Zenodo (Stovall, 2022; https://doi.org/10.5281/zenodo.7268012). The tree-level data calculated in this study are available through Figshare at https://doi.org/10.6084/m9.figshare.16652818.v1 (Stovall, 2021).

ORCID

Atticus E. L. Stovall https://orcid.org/0000-0001-9512-3318
Anthony Vorster https://orcid.org/0000-0002-0622-0683
Ryan Anderson https://orcid.org/0000-0002-2821-3302

REFERENCES

Brown, S., Schroeder, P., & Birdsey, R. (1997). Aboveground biomass distribution of US eastern hardwood forests and the use of large trees as an indicator of forest development. *Forest Ecology and Management*, *96*, 37–47. https://doi.org/10.1016/S0378-1127(97)00044-3

Calders, K., Adams, J., Armston, J., Bartholomeus, H., Bauwens, S., Bentley, L. P., Chave, J., Danson, F. M., Demol, M., Disney, M., Gaulton, R., Krishna Moorthy, S. M., Levick, S. R., Saarinen, N., Schaaf, C., Stovall, A., Terryn, L., Wilkes, P., & Verbeeck, H. (2020). Terrestrial laser scanning in forest ecology: Expanding the horizon. *Remote Sensing of Environment*, *251*, 112102. https://doi.org/10.1016/j.rse.2020.112102

Calders, K., Newnham, G., Burt, A., Murphy, S., Raumonen, P., Herold, M., Culvenor, D., Avitabile, V., Disney, M., Armston, J., & Kaasalainen, M. (2015). Nondestructive estimates of above-ground biomass using terrestrial laser scanning. *Methods in Ecology and Evolution*, *6*, 198–208. https://doi.org/10.1111/2041-210X.12301

Chave, J., Condit, R., Aguilar, S., Hernandez, A., Lao, S., & Perez, R. (2004). Error propagation and scaling for tropical forest biomass estimates. *Philosophical Transactions of the Royal Society B: Biological Sciences*, *359*, 409–420.

Chave, J., Réjou-Méchain, M., Búrquez, A., Chidumayo, E., Colgan, M. S., Delitti, W. B., Duque, A., Eid, T., Fearnside, P. M., Goodman, R. C., Henry, M., Martínez-Yrízar, A., Mugasha, W. A., Muller-Landau, H. C., Mencuccini, M., Nelson, B. W., Ngomanda, A., Nogueira, E. M., Ortiz-Malavassi, E., … Vieilledent, G. (2014). Improved allometric models to estimate the aboveground biomass of tropical trees. *Global Change Biology*, *20*, 3177–3190.

Chojnacky, D. C., Heath, L. S., & Jenkins, J. C. (2014). Updated generalized biomass equations for north American tree species. *Forestry*, *87*, 129–151. https://doi.org/10.1093/forestry/cpt053

Demol, M., Calders, K., Verbeeck, H., & Gielen, B. (2021). Forest aboveground volume assessments with terrestrial laser scanning: A ground-truth validation experiment in temperate, managed forests. *Annals of Botany*, *128*, 805–819. https://doi.org/10.1093/aob/mcab110

Demol, M., Verbeeck, H., Gielen, B., Armston, J., Burt, A., Disney, M., Duncanson, L., Hackenberg, J., Kükenbrink, D., Lau, A., Ploton, P., Sewdien, A., Stovall, A., Momo Takoudjou, S., Volkova, L., Weston, C., Wortel, V., & Calders, K. (2022). Estimating forest aboveground biomass with terrestrial laser scanning: Current status and future directions. *Methods in Ecology and Evolution*, *13*, 1628–1639. https://doi.org/10.1111/2041-210X.13906

Disney, M., Burt, A., Calders, K., Schaaf, C., & Stovall, A. (2019). Innovations in ground and airborne technologies as reference and for training and validation: Terrestrial laser scanning (TLS). *Surveys in Geophysics*. https://doi.org/10.1007/s10712-019-09527-x

Disney, M., Burt, A., Wilkes, P., Armston, J., & Duncanson, L. (2020). New 3D measurements of large redwood trees for biomass and structure. *Scientific Reports*, *10*. https://doi.org/10.1038/s41598-020-73733-6

Duncanson, L., Rourke, O., & Dubayah, R. (2015). Small sample sizes yield biased Allometric equations in temperate forests. *Scientific Reports*, *5*, 17153. https://doi.org/10.1038/srep17153

Duncanson, L. I., Dubayah, R. O., & Enquist, B. J. (2015). Assessing the general patterns of forest structure: Quantifying tree and forest allometric scaling relationships in the United States: Forest allometric variability in the United States. *Global Ecology and Biogeography*, *24*, 1465–1475. https://doi.org/10.1111/geb.12371

Friedlingstein, P., O'Sullivan, M., Jones, M. W., Andrew, R. M., Hauck, J., Olsen, A., Peters, G. P., Peters, W., Pongratz, J., Sitch, S., Le Quéré, C., Canadell, J. G., Ciais, P., Jackson, R. B., Alin, S., Aragão, L. E. O. C., Arneth, A., Arora, V., Bates, N. R., … Zaehle, S. (2020). Global carbon budget 2020. *Earth System Science Data*, *12*, 3269–3340. https://doi.org/10.5194/essd-12-3269-2020

Hackenberg, J., Wassenberg, M., Spiecker, H., & Sun, D. (2015). Non destructive method for biomass prediction combining TLS derived tree volume and wood density. *Forests*, *6*, 1274–1300.

Hopkinson, C., Chasmer, L., Young-Pow, C., & Treitz, P. (2004). Assessing forest metrics with a ground-based scanning lidar. *Canadian Journal of Forest Research*, *34*, 573–583. https://doi.org/10.1139/x03-225

Jucker, T., Caspersen, J., Chave, J., Antin, C., Barbier, N., Bongers, F., Dalponte, M., van Ewijk, K. Y., Forrester, D. I., Haeni, M., Higgins, S. I., Holdaway, R. J., Iida, Y., Lorimer, C., Marshall, P. L., Momo, S., Moncrieff, G. R., Ploton, P., Poorter, L., … Coomes, D. A. (2017). Allometric equations for integrating remote sensing imagery into forest monitoring programmes. *Global Change Biology*, *23*, 177–190. https://doi.org/10.1111/gcb.13388

Land Product Validation Subgroup (Working Group on Calibration and Validation, Committee on Earth Observation Satellites). (2021). *Aboveground woody biomass product validation good practices protocol*. https://doi.org/10.5067/DOC/CEOSWGCV/LPV/AGB.001

Lau, A., Calders, K., Bartholomeus, H., Martius, C., Raumonen, P., Herold, M., Vicari, M., Sukhdeo, H., Singh, J., & Goodman, R. C. (2019). Tree biomass equations from terrestrial LiDAR: A case study in Guyana. *Forests*, *10*, 527. https://doi.org/10.3390/f10060527

Lau, A., Martius, C., Bartholomeus, H., Shenkin, A., Jackson, T., Malhi, Y., Herold, M., & Bentley, L. P. (2019). Estimating architecture-based metabolic scaling exponents of tropical trees using terrestrial LiDAR and 3D modelling. *Forest Ecology and Management*, *439*, 132–145. https://doi.org/10.1016/j.foreco.2019.02.019

Lutz, J. A., Larson, A. J., Swanson, M. E., & Freund, J. A. (2012). Ecological importance of large-diameter trees in a temperate mixed-conifer Forest. *PLoS ONE*, *7*, e36131. https://doi.org/10.1371/journal.pone.0036131

Momo Takoudjou, S., Ploton, P., Sonké, B., Hackenberg, J., Griffon, S., de Coligny, F., Kamdem, N. G., Libalah, M., Mofack, G. I., Le Moguédec, G., Pélissier, R., & Barbier, N. (2017). Using terrestrial laser scanning data to estimate large tropical trees biomass and calibrate allometric models: A comparison with traditional destructive approach. *Methods in Ecology and Evolution*. https://doi.org/10.1111/2041-210X.12933

Picard, N., Saint-Andre, L., & Henry, M. (2012). *Manual for building tree volume and biomass allometric equations: From field measurement to prediction*. Food and Agricultural Organization of the United Nations and Centre de Coopération Internationale en Recherche Agronomique pour le Développement.

R Core Team. (2022). *R: A language and environment for statistical computing*. R Foundation for Statistical Computing.

Raumonen, P., Kaasalainen, M., Åkerblom, M., Kaasalainen, S., Kaartinen, H., Vastaranta, M., Holopainen, M., Disney, M., & Lewis, P. (2013). Fast automatic precision tree models from terrestrial laser scanner data. *Remote Sensing*, *5*, 491–520. https://doi.org/10.3390/rs5020491

Saatchi, S., Harris, N. L., Brown, S., Lefsky, M., Mitchard, E. T. A., Salas, W., Zutta, B. R., Buermann, W., Lewis, S. L., Hagen, S., Petrova, S., White, L., Silman, M., & Morel, A. (2011). Benchmark map of forest carbon stocks in tropical regions across three continents. *Proceedings of the National Academy of Sciences of the United States of America*, *108*, 9899–9904. https://doi.org/10.1073/pnas.1019576108

Stephenson, N. L., Das, A. J., Condit, R., Russo, S. E., Baker, P. J., Beckman, N. G., Coomes, D. A., Lines, E. R., Morris, W. K., Rüger, N., Álvarez, E., Blundo, C., Bunyavejchewin, S., Chuyong, G., Davies, S. J., Duque, Á., Ewango, C. N., Flores, O., Franklin, J. F., … Zavala, M. A. (2014). Rate of tree carbon accumulation increases continuously with tree size. *Nature*, *507*, 90–93. https://doi.org/10.1038/nature12914

Stovall, A. (2021). CO OHM tree allometry. *figshare*, https://doi.org/10.6084/m9.figshare.16652818.v1

Stovall, A. (2022). aestovall/OHM: Outer hull model. *Zenodo*, https://doi.org/10.5281/zenodo.7268012

Stovall, A. E. L., Anderson-Teixeira, K. J., & Shugart, H. H. (2018). Assessing terrestrial laser scanning for developing non-destructive biomass allometry. *Forest Ecology and Management*, *427*, 217–229. https://doi.org/10.1016/j.foreco.2018.06.004

Stovall, A. E. L., Shugart, H., & Yang, X. (2019). Tree height explains mortality risk during an intense drought. *Nature Communications*, *10*, 4385. https://doi.org/10.1038/s41467-019-12380-6

Stovall, A. E. L., & Shugart, H. H. (2018). Improved biomass calibration and validation with terrestrial LiDAR: Implications for future LiDAR and SAR missions. *IEEE Journal of Selected Topics in Applied Earth Observations and Remote Sensing*, *11*, 3527–3537. https://doi.org/10.1109/JSTARS.2018.2803110

Stovall, A. E. L., Vorster, A. G., Anderson, R. S., Evangelista, P. H., & Shugart, H. H. (2017). Non-destructive aboveground biomass estimation of coniferous trees using terrestrial LiDAR. *Remote Sensing of Environment*, *200*, 31–42. https://doi.org/10.1016/j.rse.2017.08.013

Vorster, A. G., Evangelista, P. H., Stovall, A. E. L., & Ex, S. (2020). Variability and uncertainty in forest biomass estimates from the tree to landscape scale: The role of allometric equations. *Carbon Balance and Management*, *15*. https://doi.org/10.1186/s13021-020-00143-6

Weinstein, B. G., Marconi, S., Bohlman, S. A., Zare, A., Singh, A., Graves, S. J., & White, E. P. (2021). A remote sensing derived data set of 100 million individual tree crowns for the national ecological observatory network. *eLife*, *10*. https://doi.org/10.7554/eLife.62922

Weiskittel, A. R., MacFarlane, D. W., Radtke, P. J., Affleck, D. L. R., Temesgen, H., Woodall, C. W., Westfall, J. A., & Coulston, J. W. (2015). A call to improve methods for estimating tree biomass for regional and national assessments. *Journal of Forestry*, *113*, 414–424.

SUPPORTING INFORMATION

Additional supporting information can be found online in the Supporting Information section at the end of this article.

How to cite this article: Stovall, A. E. L., Vorster, A., Anderson, R., & Evangelista, P. (2023). Developing nondestructive species-specific tree allometry with terrestrial laser scanning. *Methods in Ecology and Evolution*, *14*, 280–290. https://doi.org/10.1111/2041-210X.14027